J Mater Sci (2015) 50:769–776
DOI 10.1007/s10853-014-8636-y

Preparation of a gold electrode modified with Au–TiO_2 nanoparticles as an electrochemical sensor for the detection of mercury(II) ions

Lan Zhou · Wei Xiong · Shantang Liu

Received: 17 June 2014 / Accepted: 27 September 2014 / Published online: 7 October 2014

Abstract A sensitive and selective electrochemical sensor based on Au–TiO_2 nanoparticles/Chitosan/gold (Au–TiO_2 NPs/Chit/gold)-modified electrode was developed for the detection of mercury ions (Hg^{2+}), in which the composite electrode was synthesized via sol–gel method and followed by a self-assembly strategy. The morphology and microstructure of the Au–TiO_2 NPs are characterized using transmission electron microscopy and X-ray diffraction. The results demonstrate the presence of a monolayer of well-dispersed Au–TiO_2 NPs with an average size of 5–15 nm. The electrochemical properties of the resultant Au–TiO_2 NPs/Chit/gold-modified electrode and its response to Hg^{2+} are studied using cyclic voltammetry and differential pulse anodic stripping voltammetry. The operational parameters that influence the deposition and stripping, such as the supporting electrolytes, pH value, deposition potential and deposition time, are carefully studied. Under optimal conditions, the as-prepared Au–TiO_2 NPs/Chit/gold-modified electrode exhibits a wide linear response range of 5.0–400.0 nM with a correlation coefficient of 0.999. In addition, the limit of detection is 1.0 nM with a 240 s preconcentration ($S/N = 3$), which is lower than the World Health Organization and Environmental Protection Agency limits for Hg^{2+}. The practical application of the proposed method is evaluated in a real water sample, and good results are obtained. This finding is potentially important for electrochemical sensors in environmental applications.

Introduction

Heavy metal pollution has become a serious threat to human health and the environment due to the metals' high toxicities. Hg^{2+} is identified as one of the most highly toxic heavy metal ions because of its stability in contaminated sites and the complex mechanism of biological toxicity [1–3]. The harmful effects of Hg^{2+} may cause cancer, damage to the stomach, large intestine and lungs, and can also increase blood pressure and heart rate [4, 5]. Thus, it is important to develop a highly sensitive, rapid, and stable analytical method for monitoring Hg^{2+}. Currently, there are many techniques and methods for the determination of Hg^{2+}, such as (ICP-MS) [6], atomic absorption spectrophotometry (AAS) [7, 8], atomic fluorescence spectrometry (AFS) [9], X-ray fluorescence spectrophotometry (XRF) [10], and electrochemical methods [11]. Among these analytical techniques for detecting Hg^{2+}, the electrochemical methods, especially those based on metal-nanoparticle-(NP)-modified electrode materials, are some of the most commonly used because of their low cost, high sensitivity, and simple operation compared with other methods [12]. In particular, gold nanoparticles (AuNPs) are widely used in chemical sensors because of their excellent conductivity and high activity. For example, Xu and coworkers [13] prepared an AuNP-modified GCE via the electrophoretic deposition of AuNPs on a GCE surface to simultaneously determine Cd^{2+}, Pb^{2+}, Cu^{2+}, and Hg^{2+} with a low detection limit of 0.3 μM.

Ceramic nanomaterials, such as TiO_2 nanomaterials, known for their biocompatible and environmentally benign properties, have attracted considerable attention in recent years for applications in electrochemistry due to their large specific surface areas, long chemical stability, and well-aligned nanostructures [14–17]. In previous

---

L. Zhou · W. Xiong · S. Liu (✉)
School of Chemistry and Environmental Engineering, Wuhan Institute of Technology, 693 Xiongchu Road, Wuhan 430073, People's Republic of China
e-mail: liushantang@mail.wit.edu.cn

reports, Gan and coworkers [18] prepared TiO_2-graphene nanosheet nanocomposite-modified glassy carbon electrodes (GCE) as an electrochemical sensor to detect Sudan I, which exhibited a low detection limit of 0.6 nM (M = mol L^{-1}). Meanwhile, noble metal nanostructures, especially Au nanoparticles, have attracted tremendous attention in recent decades due to their excellent optical, electrochemical and electronic properties as introduced in the first paragraph. Therefore, we expect that Au–TiO_2 NPs combine the advantageous properties of these two nanomaterials, i.e., Au and TiO_2 NPs, which should endow them with unique and novel electrochemical performance. In addition, some reports have also shown that the electrocatalytic activity of TiO_2 can be enhanced by decorating its surface with noble metal nanostructures, such as Au, Pt, and Pd, due to their electrochemical and electronic properties [19–21]. Recently, Wu and coworkers [22] prepared an Au–TiO_2/GCE-modified electrode via in situ electrodepositing on TiO_2/GCE substrates and used it to detect arsenic(III), which exhibited a low detection limit of 0.04 μM. However, to the best of our knowledge, few studies have reported the use of Au–TiO_2-modified gold electrodes for the determination of Hg^{2+}.

In this paper, we report the synthesis of an Au–TiO_2 NPs/Chit/gold electrode as a sensor for the determination of Hg^{2+}. The morphology and microstructure of Au–TiO_2 NPs with a diameter of nearly 5–15 nm are characterized using TEM and XRD. The resultant Au–TiO_2 NPs/Chit/gold-modified electrode shows excellent electrochemical response toward the detection of Hg^{2+} and exhibits a wide linear response range of 5.0–400.0 nM, with a correlation coefficient of 0.999. The detection limit for Hg^{2+} is down to 1 nM with a 240 s preconcentration ($S/N = 3$). In addition, the prepared Au–TiO_2 NPs/Chit/gold-modified electrode exhibits good reproducibility and long-term stability. Therefore, we believe that the resultant modified electrode has good potential for use in electrochemical sensors in environmental applications.

Experimental

Materials

Chit was purchased from Sinopharm Chemical Regent. The following reagents $K_3Fe(CN)_6$, $K_4Fe(CN)_6$, 1 wt% $HAuCl_4$, $HgCl_2$, HAc, NaAc, KNO_3, and $NaBH_4$ were obtained from Sinopharm Chemical Reagent Ltd. A stock solution of $HgCl_2$ (1 g/l) was prepared by directly dissolving $HgCl_2$ in ultrapure water. All chemicals used in this study were of analytical grade or of the highest purity available.

Preparation of Au–TiO_2 NPs

The TiO_2 nanocomposites were prepared using a sol–gel process. Briefly, 5 mL of tetrabutyl titanate were dissolved in 70 mL of ethanol and then 3 mL of acetic acid were added. The mixed solution was stirred for 10 min, and then, 7 mL of ultrapure water was added dropwise under vigorous stirring until a white transparent sol was formed. After stirring for 24 h at room temperature, the sol transformed into a gel. The gel was dried in an oven at 105 °C and then calcinated at 500 °C for 2 h to obtain a TiO_2 powder.

The Au–TiO_2 nanocomposites were prepared by chemically reducing negatively charged $[AuCl_4]^-$ on the positively charged nano-TiO_2 surface according to a previous report with minor modifications [23]. First, a TiO_2 solution was prepared by dispersing nano-TiO_2 in the ultrapure water and sonicating for 10 min; hydrochloric acid solution was added dropwise until the pH value was approximately 1–2. Then, 0.7 mL of a 1-wt% $HAuCl_4$ solution was added to the dispersed nano-TiO_2 suspension (100 mL) with vigorous stirring. After a few hours, 0.1 mol L^{-1} of sodium borohydride was added to the solution until the solution turned purple, and Au–TiO_2 nanoparticles were synthesized.

Fabrication of the Au–TiO_2 NP/gold electrode

Prior to modification, a bare gold electrode was carefully polished with 0.3- and 0.05-μm alumina powder to a mirror surface, sonicated in absolute ethanol and ultrapure water for 5 min to remove any adsorbed substances on the electrode surface, and then dried in air. The Au–TiO_2 nanoparticles were bound to the electrode surface using Chit as a binder. The mixed solution of Au–TiO_2 and Chit was prepared by mixing 10 μL of the Au–TiO_2 solution and 2 μL of 1-mg/mL Chit with the aid of ultrasonic agitation, and then, 6 μL of the mixture were added to the surface of the gold electrode. Finally, the electrode was dried in air. In addition, a TiO_2/Chit electrode was also prepared using the same process.

Characterization

XRD patterns were obtained using a XD-5A (Shimadzu, Japan) by Cu Kα radiation at 30 kV and 30 mA. Transmission electron microscopy (TEM) images were collected using a Philips Tecnai G2 20 instrument (120 kV). Electrochemical measurements were performed using a CHI 660 electrochemical analyzer (CH Instruments, Chenhua Co. Shanghai, China) with a three-electrode electrochemical cell. An Ag/AgCl (saturated KCl) electrode and a Pt wire were used as the reference and counter electrodes, respectively, and a bare or modified gold electrode (2-mm

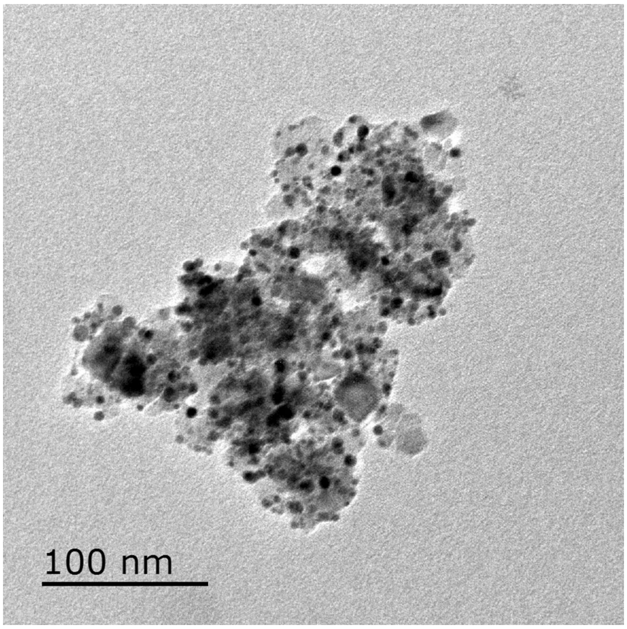

Fig. 1 TEM images of Au–TiO_2 NPs

diameter) was used as the working electrode. All measurements were made at room temperature in solutions deoxygenated with N_2 for 20 min and kept under a nitrogen atmosphere during the measurement.

Results and discussion

Characterization of the Au–TiO_2 NPs using TEM and XRD

Figure 1 shows TEM micrographs of the Au–TiO_2 nanocomposite particles. It can be observed that the AuNPs were dispersed on the TiO_2 surface and the formation of AuNPs was indicated by the dark-contrast objects that were distributed on low-contrast TiO_2, which had diameters in the range of 5–15 nm. This result indicated that Au had been grown on the TiO_2 surface and the successful formation of Au–TiO_2 nanocomposites.

The XRD patterns of the Au–TiO_2 NPs are shown in Fig. 2. The formation of Au–TiO_2 NPs was further supported by the XRD measurements. We can observe that curve a is the as-produced TiO_2, which showed a series of well-defined diffraction peaks at 25.3°, 37.9°, 48.0°, 62.8°, and 75.0° representing the (101), (004), (200), (116), and (215) crystalline planes of anatase TiO_2 (PDF$^{\#}$ 21-1272) [24], respectively. Compared with curve a, four new peaks in curve b can be observed at 38.2°, 44.4°, 64.6°, and 77.5°, which can be assigned to the (111), (200), (220), and (311) crystalline planes of gold (PDF$^{\#}$ 04-0784), matching the results of the TEM (Fig. 1) and further demonstrating that Au–TiO_2 NPs were successfully prepared in our work.

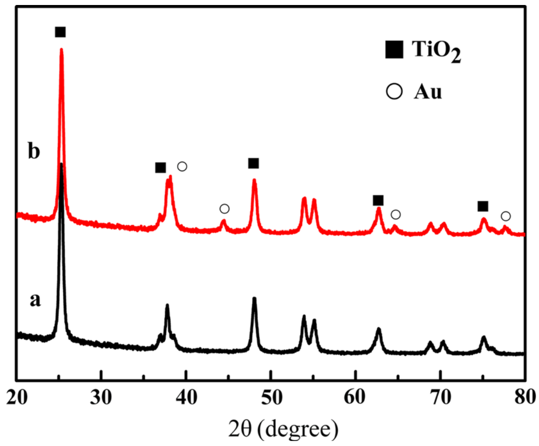

Fig. 2 XRD patterns of Au–TiO_2 NPs

Electrochemical characterization of Au–TiO_2 NPs/Chit-modified gold electrode

Cyclic voltammetry (CV) and electrochemical impedance spectrum (EIS) are commonly used for the characterization of modified electrodes and offers information about the electron-transfer kinetics of redox probes [25]. Figure 3a shows different CV profiles between the bare electrode TiO_2/Chit and Au–TiO_2/Chit-modified electrode in a solution of 0.1 M KCl, 5 mM $K_3Fe(CN)_6$, and 5 mM $K_4Fe(CN)$ at 100 mV s^{-1}. It can be observed that all curves present clear oxidation and reduction peaks. Compared with the bare electrode, the TiO_2/Chit and modified electrode have a bigger current. After the modification of the electrode using Au–TiO_2 NPs/Chit, the electrode has the highest current, as shown in curve c. In a typical EIS, the diameter of semicircle equals to the electron-transfer resistance (R_{et}). As seen in the inset of Fig. 3a, Au–TiO_2/Chit-modified electrode showed a smaller R_{et} than the bare electrode, suggesting the promotion of electron-transfer process at the modified electrode surface. These results reveal that the combination of TiO_2 and Au NPs provide easier and faster charge transfer on the electrode surface. Moreover, a comparison of the peak current obtained for different electrodes also shows that the Au–TiO_2 NP materials have been successfully modified on the bare electrode.

Figure 3b shows different DPASV profiles between the bare electrode TiO_2/Chit and Au–TiO_2/Chit-modified electrode in a solution of 0.1 M NaAc–HAc (pH 5.0) including of 0.2 μM Hg^{2+}. No peak was obtained at bare electrode. Under the same conditions, a well-defined stripping peak was found at TiO_2/Chit and Au–TiO_2/Chit-modified electrode. As shown in Fig. 3b, Au–TiO_2/Chit-

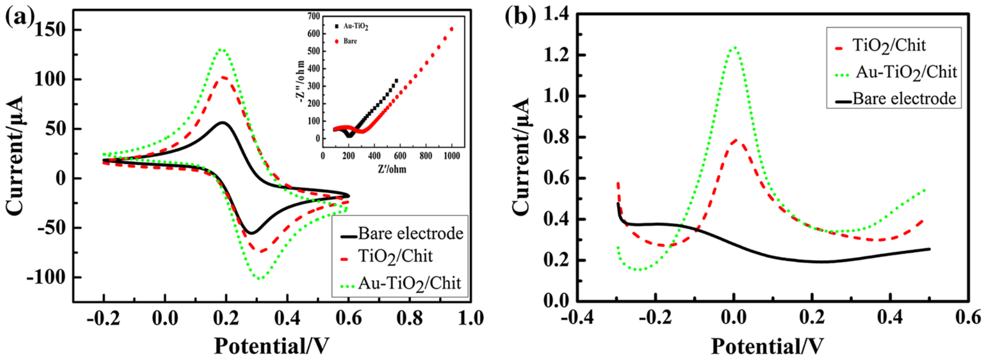

Fig. 3 CV curves (**a**) of bare electrode, TiO_2/Chit and Au–TiO_2 NPs/Chit-modified electrode in the solution of 5 mM $Fe(CN)_6^{3-/4-}$ and 0.1 M KCl, *Inset* Nyquist diagram of EIS for bare electrode and Au–TiO_2/Chit; DPASV (**b**) response of 0.2 μM Hg^{2+} on bare electrode, TiO_2/Chit and Au–TiO_2 NPs/Chit-modified electrode in the solution of in 0.1 M NaAc–HAc (pH 5.0). (Condition: deposition potential, −1.2 V; deposition time, 240 s; frequency, 20 Hz; amplitude, and 50 mV; step potential 4 mV)

modified electrode has the highest current. The increase in stripping current at this modified electrode suggested that the Au–TiO_2/Chit exhibited a good electrochemical performance toward Hg^{2+}. The anodic striping (reoxidation of metal to metal ions) of electrodeposited metal was performed at following parameters: frequency, 20 Hz; amplitude, 50 mV; and step potential, 4 mV.

Optimization of the empirical parameters

To determine the optimum experimental conditions, the effect of the experimental parameters, which includes the supporting electrolyte, pH value, deposition potential and deposition time, for a 0.2-μM Hg^{2+} solution were discussed.

Effect of the supporting electrolyte and pH value

Generally, metals have different electrochemical performance in different electrolytes [25]. Therefore, to optimize the response of the Hg^{2+} solution at Au–TiO_2 NPs/Chit gold electrode, the effect of some supporting electrolytes, such as phosphate buffer solution (PBS), acetate buffer solution (NaAc–HAc), and HCl solution, was studied using DPASV. As shown in Fig. 4a, a well-defined and highly sensitive peak was obtained when 0.1-M HAc–NaAc buffer solutions was chosen as the electrolyte. The differences from using different supporting electrolytes should be due to the metal ion complexes formed with the supporting electrolytes [25]. In addition, the mercury ion have different ion activity in the different buffers and the stripping peak potential is connected with the ion activity (α_{Hg}^{2+}) according to the Nernst equation ($E = E^0 + RT\ln\alpha/nF$), so it has the different peak potentials. Moreover, the effect of the pH in the range from 4.0 to 6.0 on the current response was also studied in 0.1-M NaAc–HAc. With an increase in the pH from 4 to 5 in Fig. 4b, the peak current gradually increased. However, the peak current decreases when the pH value is changed from 5.5 to 6.0, which may be related to the hydrolysis of the metal ions [26]. Therefore, a moderately acidic environment is important for the determination of Hg^{2+}. This result indicates that HAc–NaAc (pH 5.0) was the optimum pH value for detecting Hg^{2+}.

Deposition potential

In anodic stripping voltammetry analysis, a proper deposition potential is very important to obtain the best sensitivity. In addition, the deposition step is usually a simple and effective way to enhance the sensitivity of the sensor. Therefore, the effect of the deposition potential on the metal stripping signal was studied in the potential range from −0.2 to −1.4 V versus SCE in a 0.1-M HAc–NaAc solution at pH 5.0. As shown in Fig. 5a, the stripping currents for Hg^{2+} increased as the deposition potential shifted from −0.2 to −1.2 V and the peak current for Hg^{2+} reached a maximum at −1.2 V. However, when the potential was more negative than −1.2 V, the peak current slightly decreased, which should be mostly due to the co-hydrogen evolution at these negative potentials [27]. Although a higher peak current was obtained at −1.4 V, in order to avoid the competitive generation of H_2 and the codeposition of other metal ions from analysis of real samples, we chose −1.2 V as the optimal deposition potential for the next experiment.

Deposition time

Different deposition times can affect the detection limit and the sensitivity of the modified electrode. Thus, to choose the most appropriate deposition time, the influence of the deposition time on the stripping peak currents was also investigated from 60 to 360 s. Figure 5b shows the

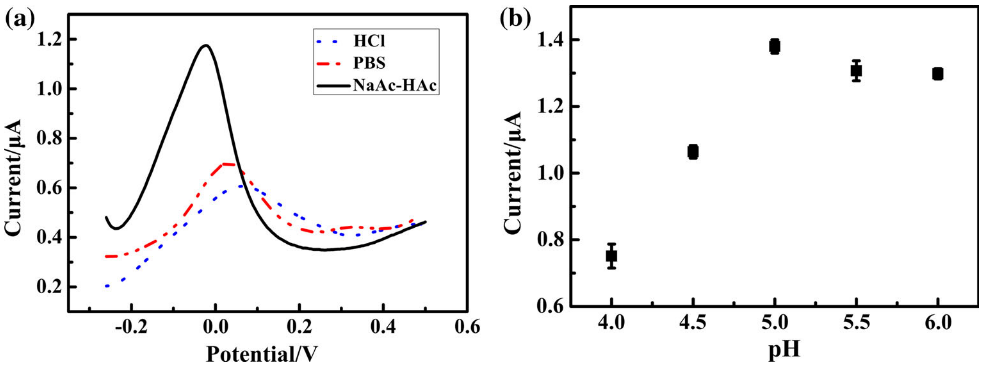

Fig. 4 Influence of **a** supporting electrolytes; **b** pH value on the voltammetric responses of the Au–TiO_2/Chit/gold electrode. (Other parameters are the same as in Fig. 3b)

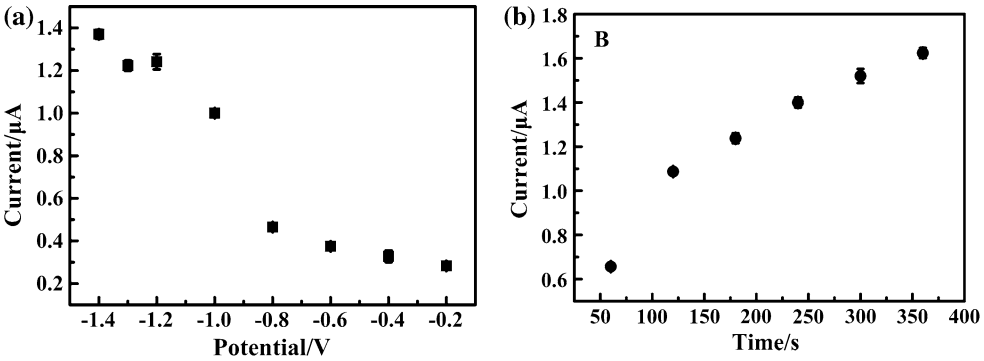

Fig. 5 Influence of **a** deposition potential and **b** deposition time on the voltammetric responses of the Au–TiO_2/Chit/gold electrode. (Supporting electrolytes: 0.1 M NaAc–HAc; pH value: 5.0 DPASV conditions are identical to those in Fig. 3b)

relationship between the peak current and the accumulation time for 0.2-μM Hg^{2+} solutions at −1.2 V. As observed from Fig. 5b, the peak current increased with deposition time. Although increasing the deposition time enhanced the sensitivity to Hg^{2+}, it also decreased the upper detection limit due to the rapid surface saturation at high concentrations of Hg^{2+} [28]. In this work, for the sake of the lower detection limit and wider response range, a deposition time of 240 s was selected for the sequencing experiments and could save analysis time.

Determination of Hg^{2+}

Using the optimized experimental conditions, differential pulse anodic stripping voltammetry (DPASV) was applied for the successive determination of Hg^{2+} at different concentrations. Figure 6 shows the DPASV responses of the Au–TiO_2 NPs/Chit/gold electrode toward Hg^{2+} in 0.1-M NaAc–HAc buffer solution (pH 5.0) over the concentrations range from 5.0 to 400.0 nM. As shown in Fig. 6, the error bars of peak current response against the concentration (inset of Fig. 6), all of the anodic stripping peak currents were proportional to the concentration of Hg^{2+}. The calibration curve and correlation coefficient were $y = 3.1328x + 0.5339$ and $R = 0.999$ (x: concentration/μmol, y: current/μA) with a preconcentration time of 240 s at the deposition potential of −1.2 V versus SCE, as shown

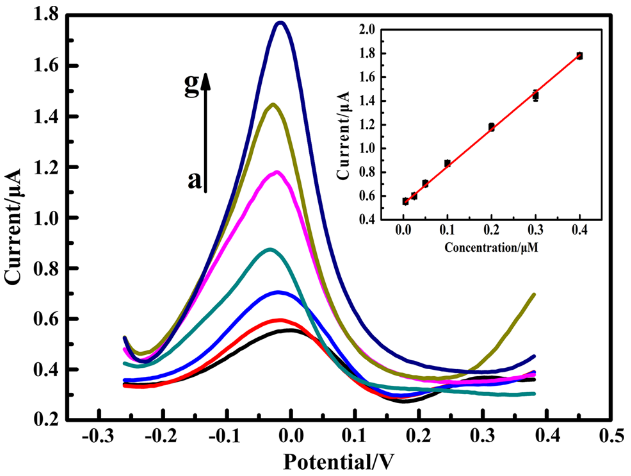

Fig. 6 DPASV responses with increasing Hg^{2+} concentration, from (*a*–*g*): 5.0×10^{-3}, 2.5×10^{-2}, 5.0×10^{-2}, 1.0×10^{-1}, 2.0×10^{-1}, 3.0×10^{-1}, 4.0×10^{-1} μM, respectively. The *inset* depicts the calibration plot of the linear relationship between the peak current and the concentration of Hg^{2+}. (Other parameters are the same as in Fig. 3b)

in the inset graph in Fig. 6. The limit of detection was calculated to be 1.0 nM (three times the background noise, $S/N = 3$) with a sensitivity of 3.133 μA μM^{-1}, which is better than or compared favorably with other reported mercury electrodes, as shown in Table 1. Moreover, the detection limit for Hg^{2+} is lower than the World Health

Table 1 Performance comparison of the modified electrode for Hg^{2+} with other electrodes

Electrode	Calibration range (μM)	Detection limit (μM)	Reference
Flake-like CuO/GCE	1–200	200	[4]
Au NPs amplified DNA/gold	–	10	[29]
Graphene-DNA/GCE	0.008–0.1	5	[30]
Surfactant-templated mesoporous silic/GCE	0.05–1	24	[31]
Au NPs/GCE	0.003–0.05	1.0	[32]
Au–TiO_2 NPs/gold	0.005–0.4	1.0	Our work

Organization (WHO) and Environmental Protection Agency (EPA) limits for Hg^{2+}. This excellent electrochemical performance toward Hg^{2+} is mainly due to the adsorption capacity of Au–TiO_2 NPs; AuNPs have a high affinity for mercury, which enhances the preconcentration effect via amalgam formation [33].

Repeatability, reproducibility, stability, and anti-interferences of electrode

The repeatability of the electrode for the determinations of target analytes was tested. The repeatability was investigated by repetitively measuring the same standard solutions of Hg^{2+}. The relative standard deviation was 5.2 % for 9 successive assays of a 0.2 μM solution of Hg^{2+}, which indicates good repeatability. In the case of reproducibility of electrodes, six electrodes were prepared. Then, the reproducibility was performed in the determination of 0.2 μM solution of Hg^{2+}. The relative standard deviation for the response between electrodes was 2.2 %, as shown in Table 2. We also examined the stability of the Au–TiO_2/Chit/gold electrode. The solution and the modified electrode were stored at room temperature for a week, and the peak currents remained stable. After a two-week storage period, the electrode retained 90 % of its initial current response. This result indicated that the composite electrode could be used for the long-term determination of Hg^{2+}. The interference of some heavy metal ions with the determination of 0.2 μM Hg^{2+} was tested under the optimal condition. It was found that 100-fold amounts of Na^+, K^+, Fe^{2+}, Cu^{2+}, Ca^{2+}, Zn^{2+}, NO_3^-, $SO_4{}^{2-}$, SCN^-, or $CO_3{}^{2-}$ have no influences on the signal from 0.2 μM Hg^{2+}. The experiment indicated that these heavy metal ions did not interfere with the determination of Hg^{2+}.

Analysis of the real samples

Water samples were used to evaluate the applicability of the proposed composite electrode for determining Hg^{2+} in real samples. The water samples were obtained directly from the university laboratory. The real samples were diluted in 0.1 M NaAc–HAc buffer solutions (pH 5.0) in a ratio of 1:1. The experimental results showed that there were no obvious signals in the samples. When Hg^{2+} was added to the real sample, a clear stripping peak can be observed. The recovery was studied by further standard additions of Hg^{2+} into the real samples to evaluate the accuracy of this method. The data measured using the electrochemical method agreed well with the spiked concentrations of the target ion (Hg^{2+}) in water, as shown in Table 3. We can see that the recovery was 98.60 and 105.75 % for the tap water samples, and the relative standard deviation of the results was in the range of 3.15–3.60 % (RSD). These results demonstrated that the proposed method has the potential for practical applications.

Table 2 Results of reproducibility test

Serial number of the electrode	1	2	3	4	5	6
Stripping peak current I_p (μA)	1.298	1.305	1.275	1.270	1.350	1.307

Table 3 Determination of Hg^{2+} in real samples

Sample	Hg^{2+} added (μM)	Hg^{2+} found (μM)	Recovery (%)	RSD (%)
Sample 1	0.050	0.0493	98.60	3.60
Sample 2	0.100	0.1057	105.75	3.15

Conclusions

In summary, a simple and sensitive electrochemical analytical method for the determination of Hg^{2+} has been developed using an Au–TiO_2-NP/Chit-modified gold electrode. The as-prepared Au–TiO_2 NPs/Chit/gold electrode has an outstanding response to Hg^{2+} due to the high electrical conductivity and large specific surface area of the Au–TiO_2 NPs. In 0.1-M NaAc–HAc buffer solutions (pH 5.0), this modified electrode showed a wide linear current response toward Hg^{2+} in the concentration range from 5.0 to 400.0 nM with a detection limit of 1.0 nM ($S/N = 3$), which provided a new sensitive electrode for the detection of Hg^{2+}. In addition, the reproducibility and stability measurements demonstrated that the Au–TiO_2 NPs/Chit/gold electrode has excellent stability, reproducibility, sensitivity, and electrocatalytic activity for the determination of Hg^{2+}. Furthermore, the practical application of the proposed method is evaluated in real water samples, and good results were obtained. This study highlights the potential of Au–TiO_2-NP-modified gold electrodes as electrochemical sensors for applications in environmental control.

Acknowledgements The project was supported by the National Natural Science Foundation of China (No. 21071113), the Natural Science Foundation of Hubei Province (No. 2011CDA049), the International Cooperation Foundation of Hubei Province (No. 2012IHA00201), and the Scientific Innovation Team Project of the Hubei Provincial Department of Education (T201306).

References

1. Peng QM, Guo JX, Zhang QR, Xiang JY, Liu BZ, Zhou AG, Liu RP, Tian YJ (2014) Unique lead adsorption behavior of activated hydroxyl group in two-dimensional titanium carbide. J Am Chem Soc 136:4113–4116
2. Wang QR, Kim D, Dionysiou DD, Sorial GA, Timberlake D (2004) Sources and remediation for mercury contamination in aquatic systems: a literature review. Environ Pollut 131:323–336
3. Rajabi HR, Roushani M, Shamsipur M (2013) Development of a highly selective voltammetric sensor for nanomolar detection of mercury ions using glassy carbon electrode modified with a novel ion imprinted polymeric nanobeads and multi-wall carbon nanotubes. J Electroanal Chem 693:16–22
4. Wu ZC, Jiang LD, Chen HM, Xu HR, Wang XH (2012) Synthesis of folding flake-like CuO sub-microstructure and its application on mercury(II) sensor. J Mater Sci 23:858–864. doi:10.1007/s10854-011-0506-7
5. Chen D, Hu B, Huang C (2009) Chitosan modified ordered mesoporous silica as micro-column packing materials for on-line flow injection-inductively coupled plasma optical emission spectrometry determination of trace heavy metals in environmental water samples. Talanta 78:491–497
6. Lee JM, Boyle EA, Echegoyen-Sanz Y, Fitzsimmons JN, Zhang RF, Kayser RA (2011) Analysis of trace metals (Cu, Cd, Pb, and Fe) in seawater using single batch nitrilotriacetate resin extraction and isotope dilution inductively coupled plasma mass spectrometry. Anal Chim Acta 686:93–101
7. PohL P (2009) Determination of metal content in honey by atomic absorption and emission spectrometries. Trends Anal Chem 28:117–128
8. Rofouei M, Sabouri M, Ahmadalinezhad A (2011) A solid phase extraction of ultra traces mercury(II) using octadecyl silica membrane disks modified by 1,3-bis(2-ethoxyphenyl)triazene (EPT) ligand and determination by cold vapor atomic absorption spectrometry. J Hazard Mater 192:1358–1363
9. Gasperi J, Garnaud S, Rocher V, Moilleron R (2008) Priority pollutants in wastewater and combined sewer overflow. Sci Total Environ 407:263–272
10. Marguí E, Kregsamer P, Hidalgo M, Tapias J, Queralt I, Streli C (2010) Analytical approaches for Hg determination in wastewater samples by means of total reflection X-ray fluorescence spectrometry. Talanta 82:821–827
11. Safavi A, Farjami E (2011) Construction of a carbon nanocomposite electrode based on amino acids functionalized gold nanoparticles for trace electrochemical detection of mercury. Anal Chim Acta 688:43–48
12. Cui L, Wu J, Li J, Ge YQ, Ju HG (2014) Electrochemical detection of Cu^{2+} through Ag nanoparticle assembly regulated by copper-catalyzed oxidation of cysteamine. Biosens Bioelectron 55:272–277
13. Xu XX, Duan GT, Li Y, Liu GQ, Wang JJ, Zhang HW, Dai ZF, Cai WQ (2014) Fabrication of gold nanoparticles by laser ablation in liquid and their application for simultaneous electrochemical detection of Cd^{2+}, Pb^{2+}, Cu^{2+}, Hg^{2+}. ACS Appl Mater Interfaces 6:65–71
14. Wen L, Liu B, Zhao X, Nakata K, Fujishima A (2013) Pretreating sputtered TiO_2 film by photoelectrocatalysis to increase the performance of photo-activity and photoinduced hydrophilicity. J Electroanal Chem 688:224–227
15. Zhang Q, Xu H, Yan W (2012) Fabrication of a composite electrode: CdS decorated Sb–SnO_2/TiO_2–NTs for efficient photoelectrochemical reactivity. Electrochim Acta 61:64–72
16. Hosseini MG, Momeni MM (2012) Platinum nanoparticle-decorated TiO_2 nanotube arrays as new highly active and non-poisoning catalyst for photo-electrochemical oxidation of galactose. Appl Catal A 427–428:35–42
17. Primo A, Corma A, Gracia H (2011) Titania supported gold nanoparticles as photocatalyst. Phys Chem Chem Phys 13:886–910
18. Gan T, Sun JY, He MM, Wang LL (2014) Highly sensitive electrochemical sensor for Sudan I based on graphene decorated with mesoporous TiO_2. Ionics 20:89–95
19. Chanmanee W, de Tacconi NR, Rajeshwar K, Lin WY, Nikiel L, Wampler WA (2012) Photocatalytically generated trimetallic (Pt–Pd–Au/C–TiO_2) nanocomposite electrocatalyst. J Electrochem Soc 159:F226–F233
20. Xing Y, Cai Y, Vukmirovic MB, Zhou WP, Karan H, Wang JX, Adzic RR (2010) Enhancing oxygen reduction reaction activity via Pd–Au alloy sublayer mediation of Pt monolayer electrocatalysts. J Phys Chem Lett 1:3238–3242
21. Lin C, Song Y, Cao LX, Chen SW (2013) Oxygen reduction catalyzed by Au–TiO_2 nanocomposites in alkaline media. ACS Appl Mater Interfaces 5:13305–13311
22. Wu J, Yang M, Xiao J, Fu XC, Jin JC, Li LG, Chang WG, Xie CG (2013) Gold nanoparticle dropped titania microsphere hybrids as an enhanced sensitive material for stripping voltammetry determination of As(III). J Electrochem Soc 160:B225–B230
23. Wei M, Liu Y, Gu ZZ, Liu ZD (2011) Electrochemical Detection of catechol on boron-doped diamond electrode modified with Au/TiO_2 nanorod composite. J Chin Chem Soc 58:516–521
24. Tian W, Fan XY, Yang HS, Zhang XB (2010) Preparation of MnO_x/TiO_2 composites and their properties for catalytic oxidation of chlorobenzene. J Hazard Mater 177:887–891
25. Xu RX, Yu XY, Gao C, Jing YJ, Han DD, Liu JH, Huang XJ (2013) Non-conductive nanomaterial enhanced electrochemical response in stripping voltammetry: the use of nanostructured magnesium silicate hollow spheres for heavy metal ions detection. Anal Chim Acta 790:31–38
26. Wei Y, Gao C, Meng FL, Li HH, Wang L, Liu JH, Huang XJ (2012) SnO_2/reduced graphene oxide nanocomposite for the simultaneous electrochemical detection of Cadmium(II), Lead(II), Copper(II), and Mercury(II): an interesting favorable mutual interference. J Phys Chem C 116:1034–1041
27. Gao XH, Wei WZ, Yang L, Guo ML (2006) Carbon nanotubes/poly(1,2-diaminobenzene) nanoporous composite film electrode prepared by multipulse potentiostatic electropolymerisation and its application to determination of trace heavy metal ions. Electroanalysis 18:485–492
28. Wei Y, Yang R, Liu JH, Huang XJ (2013) Selective detection toward Hg(II) and Pb(II) using polypyrrole/carbonaceous nanospheres modified screen-printed electrode. Electrochim Acta 105:218–223
29. Miao P, Liu L, Li Y, Li G (2009) A novel electrochemical method to detect mercury(II) ions. Electrochem Commun 11:1904–1907

30. Zhang Y, Zhao H, Wu ZJ, Xue Y, Zhang XF, He YJ, Li XJ, Yuan ZB (2013) A novel graphene-DNA biosensor for selective detection of mercury ions. Biosens Bioelectron 48:180–187
31. Sanchez A, Walcarius A (2010) Surfactant-templated sol–gel silica thin films bearing 5-mercapto-1-methyl-tetrazole on carbon electrode for Hg(II) detection. Electrochim Acta 55: 4201–4207
32. Abollino O, Giacomino A, Malandrino M, Marro S, Mentasti E (2009) Voltammetric determination of methylmercury and inorganic mercury with an home made gold nanoparticle electrode. J Appl Electrochem 39:2209–2216
33. Ordeig O, Banks CE, del Campo J, Muñoz FX, Compton RG (2006) Trace detection of Mercury(II) using gold ultra-microelectrode arrays. Electroanalysis 18:573–578